



## Research paper

# Stability analysis of heavy machinery moving on weak subsoil. 3D FEM model vs. analytical models

Aleksander Urbański<sup>1</sup>, Mateusz Richter<sup>2</sup>

**Abstract:** In this paper, the authors present an extension of the scope of the previously conducted research to the full three-dimensional computer simulation (using the finite element method), which takes into account the interaction between: heavy caterpillar tracks system – working platform – weak subsoil. The article presents a computer model considering two caterpillars, resting on elastic-plastic sub-soil, with standard Mohr-Coulomb yield conditions, allowing for computer simulation of the behavior of the system up to achievement of ultimate limit state. The results of the above model are treated as the reference for a simplified Analytical Models of estimating the limit state, which might be used in design procedures. In turn, these Analytical Models are enhancements of previously presented one. The most important results concluding from the Analytical Model are simple interaction formulas, in the space of moments acting on the machine-subsoil system, limiting a domain of safety in given soil conditions.

**Keywords:** 3D FEM model, analytical models, geotechnical engineering, interaction curves, subsoil – machine interaction, working platform

<sup>1</sup>DSc., PhD., Eng., Assistant professor, Cracow University of Technology, Faculty of Environmental Engineering and Energy, ul. Warszawska 24, 31-155 Krakow, Poland, e-mail: [aurbansk@pk.edu.pl](mailto:aurbansk@pk.edu.pl), ORCID: [0000-0002-5544-9134](https://orcid.org/0000-0002-5544-9134)

<sup>2</sup>PhD., Eng., University of Agriculture in Krakow, Department of Rural Building, Al. Mickiewicza 24/28, 59-130 Krakow, Poland, e-mail: [mateusz.richter@urk.edu.pl](mailto:mateusz.richter@urk.edu.pl), ORCID: [0000-0001-6813-5364](https://orcid.org/0000-0001-6813-5364)

## 1. Introduction

The assessment of the stability of heavy working machines operating on various soils is a significant problem that often occurs in geotechnical engineering. When using the term “stability”, it should be emphasised that in this case it concerns the loss of balance of a heavy tracked machine moving on the ground caused by insufficient bearing capacity of the subsoil. Stability is considered in two aspects: the scientific aspect and the aspect related to the safety of the immediate surroundings of the heavy machinery. In practical terms, the research problem concerns disasters related to the overturning of construction machines on construction sites, while in theoretical terms it is considered as an interaction problem of a construction machine – a working platform – weak subsoil. The working platform is an earth structure prepared and verified in terms of load capacity, temporary or permanent, made on the native soil base of coarse-grained or stabilized aggregates, constituting a surface for setting up and operating heavy construction equipment, machines and devices in a safe manner. Computer simulations of the load-bearing capacity of sand layers lying above the clay subsoil when the sand layer thickness  $H$  is comparable with the foundation width  $B$  (equal to the track width of a construction machine) were discussed by Burd and Frydman [1]. In the work [2] by Michałowski and Shi, the bearing capacity of a two-layer (the upper layer consisting of sand and the lower layer consisting of clay) of the subsoil on which the direct foundation is placed was taken into account. Considerations regarding the failure mechanism characteristic of a two-layer soil, where the upper layer is medium or dense sand, and the lower layer is soft clay (weak subsoil), are presented in [3, 4] and [5]. In these studies, the spatial variability of the subsoil strength parameters is considered only in soft clay. It was assumed that the strength parameters of the upper layer (sand layer) are constant. This scenario is adequate to the problem of working platforms. Numerical studies on the multilayer subsoil have been the subject of numerous studies [6–18]. Thus, in the authors opinion, the basic result of these works, the bearing capacity of a strip foundation  $q$  [force/length<sup>2</sup>], is well recognized, and can be adopted as a fundamental entry parameter to be used in the analytical models developed in this research. The proposed models are limited only to the estimation of the bearing capacity and are not devoted to the serviceability limit states, which are found in the works of other researchers [19, 20].

Recent work is the continuation of the previous work of the authors [21–23] dealing with some partial problems. Here, a final solution of the problem of achieving limit state of loss of stability for a system machine-subsoil is given (analytical and numerical approach). The original elements are listed in final conclusion (point 5)

In the works [21–23] on the interaction of heavy caterpillar tracks system – subsoil, the following models were made: 3D FEM model  $\frac{1}{2}$ (simulation of only one caterpillar, using symmetry of the system), Approximation Model (approximation of results of 3D FEM model  $\frac{1}{2}$ using the approximating equations), Analytical Model (closed solution without the use of time-consuming computer simulations). In the further part of the work, studies of a computer model including full simulations of the crawler construction machine – subsoil interaction are presented. In each of the studies to date (in the 3D FEM model as well as analytical models), the parameters for the calculations (geometrical data, dead weight of the machine)

were characteristic of the Bauer BG20H / BT60 piling machine, often used on construction sites [24].

Basing assumptions made for both classes of mechanical models (analytical and numerical) of the analysed machine-subsoil system are the following:

- The machine is moving on a caterpillar tracks system (exclusively). Machines moving on wheels are not considered in this article.
- The whole machine, including its two caterpillar tracks, is treated as a perfectly rigid body.
- The distribution of all individual masses of the components of the construction machine (chassis, body, mast, etc.) is known. This means that it is possible to at least approximately calculate the coordinates of each center of mass of the individual elements and the corresponding moments of inertia.
- The subsoil is treated as an elastic perfectly plastic continuum in which Mohr-Coulomb (M-C) yield criterion is used. It is characterised by two strength parameters i.e. friction angle  $\phi$  and cohesion  $c$  for fully drained conditions; in case of impermeable soils it can be reduced to the Tresca model in which undrained shear strength  $s_u$  is used as an unique strength parameter. This is the simplest choice, recommended by majority of design standards (i.e. Eurocode EC 7) for the limit state of bearing capacity of a subsoil.
- The impact of local unevenness in the distribution of contact stress under the caterpillar is ignored.

Numerical analysis of the problem requires a solution of unilateral contact problem. Basic theory and algorithms of this problem may be found in references [25–27].

## 2. Analytical models

The Analytical Model in its basic version was presented in the work [21]. The following modifications are made to specify the basic Analytical Model due to:

- variable length of the contact zone in the limit state,
- independent mechanism of the loss of stability due to rotation only in the YZ plane,
- unequal ground bearing capacity under each of the caterpillar.

### 2.1. Limit state for the two caterpillar tracks system

The equations for the displacement of the track center and the angle of rotation based on the force distribution were derived in detail in the earlier work [21]. They lead to the shape of contact stresses in the ultimate state accompanying loss of stability by the rotation of the machine which are shown in Fig. 2 and Fig. 3. The following basic relations of simple statics of the system and also symbolics are given in a manner similar to this given in works [21–23]. Due to the possibility of uneven load transmitted by the tracked undercarriage to the ground, the dimensionless load distribution coefficient was introduced  $\xi_i = \frac{Q_i}{Q}$ ,  $i = 1, 2$ .

The equilibrium of a system of two tracks loaded with vertical forces  $Q_1 = \xi \cdot Q$  is considered and  $Q_2 = (1 - \xi) \cdot Q$  where  $Q$  is the total weight of the machine. The  $M_X$ ,  $M_Y$

moments acting on the machine correspond to the  $M_i$  moments acting on individual caterpillars. Introduced are dimensionless eccentricities  $e_i = \frac{2 \cdot M_i}{Q_i \cdot L}$ ,  $i = 1, 2$ ,  $e_X = \frac{2 \cdot M_X}{Q \cdot L}$  and  $e_Y = \frac{2 \cdot M_Y}{Q \cdot D}$ , where:  $D$  – track spacing [m],  $L$  – track length [m] and  $B$  – track width [m]. Following relationships result from the equivalence of force systems:  $(Q, M_X, M_Y) \equiv (Q_1, Q_2)$

$$(2.1) \quad e_X(\xi) = \xi \cdot e_1 + (1 - \xi) \cdot e_2$$

$$(2.2) \quad e_Y(\xi) = 2 \cdot \xi - 1$$

The static scheme (loads) is shown in Fig. 1.

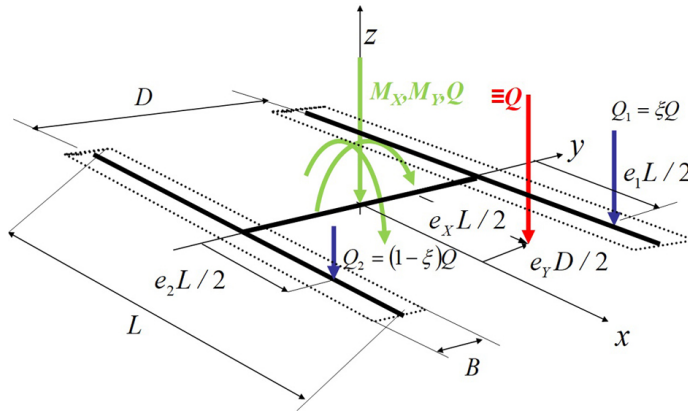


Fig. 1. Static scheme of a heavy caterpillar tracks system

The relationship between eccentricities  $e_i$  and load capacity indicator for the single caterpillar track  $p_i$  ( $0 < p_i < 1$ ):  $p_i = Q_i / N$ ,  $i = 1, 2$ , where  $N$  is the bearing capacity of the subsoil designated for a single track takes the form, coming from limit state equilibrium is:

$$(2.3) \quad p_i = 1 - e_i$$

By introducing a factor of utilisation of the total bearing capacity of the system subsoil:

$$(2.4) \quad \eta = \frac{Q}{2N} = \frac{Q}{2\hat{q} \cdot BL}, \quad \eta \in (0, 1),$$

where  $\hat{q}$  is limit load capacity of the subsoil, see Eq. (2.8), we can create a system of equations:

$$(2.5) \quad \begin{cases} (1 - e_1) - 2\xi\eta = 0, \\ (1 - e_2) - 2(1 - \xi)\eta = 0. \end{cases}$$

from which, after eliminating  $\xi$  and using relations (2.1), (2.2) we obtain the basic formula for determining the interaction curves

$$(2.6) \quad e_X = 1 - (1 + e_Y^2) \cdot \eta$$

assuming the same bearing capacity of the subsoil under both tracks.

### 2.2. Variable length of the contact zone in the limit state

New research on the Analytical Model, which was not presented in the work [22], concerns dependence of the bearing capacity on the variable length of the contact zone in the limit state. In the case of increasing value of the eccentricity of the force loading the track, the track is detached from the subsoil, which reduces the length of the contact zone ( $L'$ ) in relation to the unreduced (basic) track length ( $L$ ). Evidence of the formula (2.7) resulting from the balance of forces acting on one caterpillar track in a limit state is shown in Fig. 2.

$$(2.7) \quad L' = (1 - e)L$$

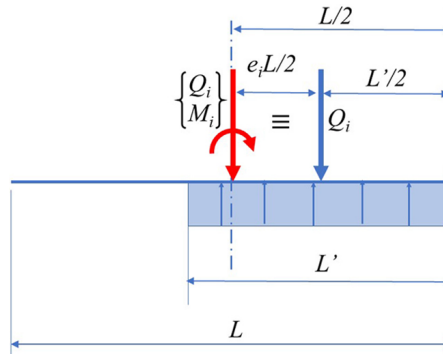


Fig. 2. Forces decomposition in limit state

If the shape factors modifying bearing capacities  $q_c, q_\gamma$  established for infinitely long strip included in the EC7 [28] standard are considered, the limit load capacity of the subsoil takes the form:

$$(2.8) \quad \hat{q} = q_c \cdot s_c + q_\gamma \cdot s_\gamma$$

with the bearing resistance factors  $N_c, N_\gamma, N_d$  and  $s_c, s_\gamma$  shape correction coefficients,  $c$  – cohesion,  $\Phi$  – internal friction angle and  $\gamma$  – unit weight.

$$(2.9) \quad q_c = c \cdot N_c$$

$$(2.10) \quad q_\gamma = \frac{1}{2} \cdot \gamma \cdot B \cdot N_\gamma$$

$$(2.11) \quad N_c = (N_d - 1) \cdot \tan^{-1}(\Phi), \quad \text{if } \Phi = 0 \Rightarrow N_c = 2 + \pi$$

$$(2.12) \quad N_d = e^{\pi \tan \varphi} \tan^2 \left( \frac{\pi}{4} + \frac{\Phi}{2} \right)$$

$$(2.13) \quad N_\gamma = 2(N_d - 1) \cdot \tan(\Phi)$$

$$(2.14) \quad s_c = 1 + \frac{0.2B}{L'} = 1 + \frac{\lambda_c}{1 - e}, \quad \lambda_c = 0.2 \frac{B}{L}$$

$$(2.15) \quad s_\gamma = 1 - \frac{0.3B}{L'} = 1 - \frac{\lambda_\gamma}{1 - e}, \quad \lambda_\gamma = 0.3 \frac{B}{L}$$

Load capacity indicator for the single caterpillar track  $p_i$  due to modified bearing capacity of the subsoil  $\hat{q}$  is:

$$(2.16) \quad p_i = \frac{Q_i}{B \cdot L \cdot (q_c \cdot s_c + q_\gamma \cdot s_\gamma)} = \frac{Q_i}{N_\infty [(1-f) \cdot s_c + f \cdot s_\gamma]}$$

where  $N_\infty = (q_c + q_\gamma)BL$  is bearing capacity determined for the infinite length of the track ( $L \rightarrow \infty$ ) and  $f$  is dimensionless factor:

$$(2.17) \quad f = \frac{q_\gamma}{q_c + q_\gamma}, \quad 1 - f = \frac{q_c}{q_c + q_\gamma}$$

The system of equations describing the interaction of both tracks of the system, considering Eq. (2.3) can be put as:

$$(2.18) \quad \begin{cases} 1 - e_1 = \frac{2 \cdot \xi \cdot \eta}{(1-f) \cdot \left(1 + \frac{\lambda_c}{1-e_1}\right) + f \cdot \left(1 - \frac{\lambda_\gamma}{1-e_1}\right)} \\ 1 - e_2 = \frac{2 \cdot (1-\xi) \cdot \eta}{(1-f) \cdot \left(1 + \frac{\lambda_c}{1-e_2}\right) + f \cdot \left(1 - \frac{\lambda_\gamma}{1-e_2}\right)} \end{cases}$$

After further transformations:

$$(2.19) \quad \begin{cases} 2 \cdot \xi \cdot \eta = 1 - e_1 - (f \cdot (\lambda_c + \lambda_\gamma) - \lambda_c) \\ 2 \cdot (1-\xi) \cdot \eta = 1 - e_2 - (f \cdot (\lambda_c + \lambda_\gamma) - \lambda_c) \end{cases}$$

In order to simplify the notation, we introduce a total correction factor related to the change of the length of the track contact zone  $\lambda$ , equal to:

$$(2.20) \quad \lambda = f \cdot (\lambda_c + \lambda_\gamma) - \lambda_c$$

After substituting equations (2.12), (2.13) to (2.17), we obtain equation (2.20) which reduces to the expression:

$$(2.21) \quad \lambda = \frac{\frac{1}{2} \cdot \gamma \cdot B \cdot N_\gamma \cdot \lambda_\gamma - N_c \cdot c \cdot \lambda_c}{N_c \cdot c + \frac{1}{2} \cdot \gamma \cdot B \cdot N_\gamma}$$

Finally, also inserting (2.20) into equation (2.19) we get:

$$(2.22) \quad \begin{cases} e_1 = 1 - 2 \cdot \xi \cdot \eta - \lambda \\ e_2 = 1 - 2 \cdot (1-\xi) \cdot \eta - \lambda \end{cases}$$

Proceeding analogously to deriving the final expression into the interaction curves in the basic Analytical Model, after substituting equation (2.22) to equations (2.1), (2.2) we obtain the following relationships:

$$(2.23) \quad \begin{cases} \xi \cdot (1 - 2 \cdot \xi \cdot \eta - \lambda) + (1-\xi) \cdot (1 - 2 \cdot (1-\xi) \cdot \eta - \lambda) = e_X \\ 2 \cdot \xi - 1 = e_Y \end{cases}$$

Equation (2.24) after simplification and elimination the variable  $\xi$ , leads to sought equation describing the interaction curve taking into account the variable length of the contact zones in the limit state:

$$(2.24) \quad e_X = 1 - \left(1 + e_Y^2\right) \cdot \eta - \lambda$$

After transformation, it allows us to obtain the coefficient  $\eta$  in a form:

$$(2.25) \quad \eta = \frac{1 - e_X - \lambda}{1 + e_Y^2}$$

### EXAMPLE

In each of the examples, data such as total weight  $Q$  of the machine, geometrical parameters  $B$ ,  $D$ ,  $L$  of the track system were used as for the Bauer BG20H/BT60 piling machine.

Assuming that the track width –  $B = 0.7$  m, track length –  $L = 4.7$  m partial correction factor  $\lambda_C$ ,  $\lambda_Y$  take the form:  $\lambda_C = 0.2 \cdot \frac{0.7 \text{ m}}{4.7 \text{ m}} = 0.03$  [-],  $\lambda_Y = 0.3 \cdot \frac{0.7 \text{ m}}{4.7 \text{ m}} = 0.045$  [-].

Based on research work [22], we follow the idea presented in Bowles [26], of taking the weighted average of parameters  $c_{av}$ ,  $\Phi_{av}$ ,  $\gamma_{av}$  of the full set of layers up to the depth  $H = 2B$ , with its thickness  $h_i$  being the corresponding weighting factors. Szypcio and Dołżyk [30] used the method from [29] to determine the ultimate bearing capacity of the layered subsoil. An “indirect” formula is recommended in [29], [30] for averaging friction angle, i.e. for  $\tan(\Phi_{av})$ , instead of  $\Phi_{av}$  alone. For the “weak” case it gives:

$$\left. \begin{aligned} \gamma_{av} &= \frac{0.5 \cdot 18 + 0.6 \cdot 17 + 0.3 \cdot 18}{1.4} = 17.57 \frac{\text{kN}}{\text{m}^3} \\ c_{av} &= \frac{0.5 \cdot 5 + 0.6 \cdot 30 + 0.3 \cdot 5}{1.4} = 15.7 \text{ [kPa]} \\ \tan \Phi_{av} &= \frac{0.5 \cdot \tan 32^\circ + 0.6 \cdot 0 + 0.3 \cdot \tan 32^\circ}{1.4} \rightarrow \Phi_{av} = 19.65^\circ \end{aligned} \right\}.$$

Bearing capacity factors take values:

$$N_d = e^{\pi \cdot \tan(19.65)} \cdot \tan^2 \left( 45 + \frac{19.65}{2} \right) = 6.18 \text{ [-]}, \quad N_c = (N_d - 1) \cdot \tan^{-1}(19.65) = 14.511 \text{ [-]}$$

$$N_\gamma = 2 \cdot (N_d - 1) \cdot \tan(19.65) = 3.7 \text{ [-]}$$

Using EC7 [28] standard equation  $\hat{q}_\infty = q_{\infty c} + q_{\infty \gamma} = N_c \cdot c + 0.5 N_\gamma \gamma B$  we get:  $\hat{q}_{\text{weak}} = 14.511 \cdot 15.7 + 0.5 \cdot 3.7 \cdot 17.57 \cdot 0.7 = 250$  kPa. Using equation (2.4) for total weight of heavy machine  $Q = 725$  kN and “weak” subsoil we get:  $\eta_{\text{weak}} = \frac{725}{2 \cdot 250 \cdot 0.7 \cdot 4.7} = 0.44$  [-] Total correction factor  $\lambda$  for “weak” subsoil takes the form:

$$\lambda = \frac{\frac{1}{2} \cdot 17.57 \cdot 0.7 \cdot 3.7 \cdot 0.045 - 14.511 \cdot 15.7 \cdot 0.03}{14.511 \cdot 15.7 + \frac{1}{2} \cdot 17.57 \cdot 0.7 \cdot 3.7} = -0.023 \text{ [-]}$$

Summarising, the data for the Analytical Models (with total correction factor  $\lambda$ ) are given in Table 1.

The results of calculations with correction factor  $\lambda$  are shown in Fig. 9.

Table 1. Parameters of the Analytical Model (with total correction factor  $\lambda$ )

Parameter	Units	Model 1 – “Weak”	Model 2 – “Strong”
$\lambda_C$	[-]	0.03	0.03
$\lambda_\gamma$	[-]	0.045	0.045
$\gamma_{av}$	$\frac{\text{kN}}{\text{m}^3}$	17.57	18
$c_{av}$	[kPa]	15.7	0
$\Phi_{av}$	[deg]	19.65	32
$N_c$	[-]	14.511	35.49
$N_\gamma$	[-]	3.7	27.715
$N_d$	[-]	6.181	23.177
$\hat{q}_\infty$	[kPa]	250	352
$\eta$	[-]	0.441	0.314
$\lambda$	[-]	<b>-0.023</b>	<b>0.045</b>

### 2.3. Second, independent failure mechanism (rotation only in the YZ plane)

Considering the particular case of  $e_X = 0$  in the Analytical Model, description of the mechanism of failure due to deformation of the subsoil under only one track, leading to rotation exclusively around the X axis (in the YZ plane) appears. Assuming that in the first equation of the system (2.5)  $e_1 = 0$  ( $e_X = 0$ ), it takes the form:

$$(2.26) \quad 1 - \frac{\xi \cdot Q}{N} = 0$$

which after substituting equation (2.4) and using expression  $\xi = \frac{1 + e_Y}{2}$  leads to the equation:

$$(2.27) \quad 1 - 2 \cdot \left( \frac{1 + e_Y^{\text{lim}}}{2} \right) \cdot \eta = 0$$

and allows to evaluate limiting value of the eccentricity  $e_Y$  in the ultimate limit state:

$$(2.28) \quad e_Y^{\text{lim}} = \frac{1}{\eta} - 1$$

The conclusion is that the limit values of the eccentricity  $e_Y^{\text{lim}}$  appear for the value of  $\eta > 0.5$ , and this failure mechanism would be predominant if  $e_Y \geq e_Y^{\text{lim}}$ .

### 2.4. Ultimate state in the case of uneven bearing capacities of subsoil

The aim of this section is to derive interaction curves in the ( $e_X, e_Y$ ) space analogously to the manner of sections 2.1–2.2, for the case when each of the caterpillars rests on the subsoil with different values of the ultimate bearing capacity. Force distribution accompanying limit state is shown in Fig. 3.



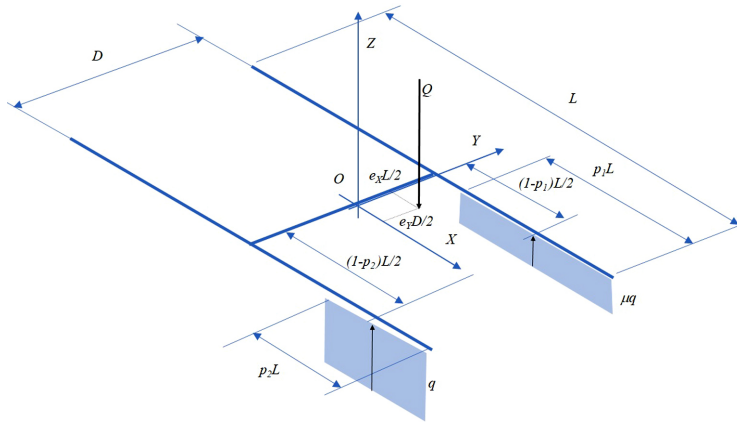


Fig. 3. Force distribution in the limit state with uneven bearing capacities of subsoil for each of the caterpillars

The basic system of equilibrium equations takes the form:

$$\begin{aligned}
 (2.29) \quad & p_1 \cdot \mu q \cdot L + p_2 \cdot q \cdot L = Q \\
 (2.30) \quad & p_1 \cdot \mu q \cdot L \cdot \left( \frac{L - L \cdot p_1}{2} \right) + p_2 \cdot q \cdot L \cdot \left( \frac{L - L \cdot p_2}{2} \right) = M_X \\
 (2.31) \quad & p_1 \cdot \mu q \cdot L \cdot \frac{D}{2} - p_2 \cdot q \cdot L \cdot \frac{D}{2} = M_Y
 \end{aligned}$$

In it, coefficient  $0 < \mu < 1$  is the ratio between the bearing capacities of the subsoil under individual tracks. Using the relations:  $M_X = e_x \cdot \frac{QL}{2}$ ,  $M_Y = e_y \cdot \frac{QD}{2}$ , then multiplying equation (2.30) by  $\frac{2}{L^2 \cdot q}$ , multiplying equation (2.31) by  $\frac{2}{L \cdot D \cdot q}$  and noting that temporary factor of utilisation of the total bearing capacity of the system  $\eta = \frac{Q}{2 \cdot L \cdot q}$  is taken as if it is related to the subsoil with greater bearing capacity, the equilibrium equations are rewritten in dimensionless form:

$$\begin{aligned}
 (2.32) \quad & \mu \cdot p_1 + p_2 = 2\eta \\
 (2.33) \quad & \mu \cdot p_1 \cdot (1 - p_1) + p_2 \cdot (1 - p_2) = 2e_x \cdot \eta \\
 (2.34) \quad & \mu \cdot p_1 - p_2 = 2e_y \cdot \eta
 \end{aligned}$$

Eliminating load capacity indicators  $p_1, p_2$ , gives equation (2.35), which, after conversion, leads to the sought formula (2.36) for the interaction curve in a case of uneven bearing capacities of subsoil:

$$\begin{aligned}
 (2.35) \quad & \mu \cdot \left( \frac{\eta \cdot (1 + e_y)}{2 \cdot \mu} \right) \cdot \left( 1 - \left( \frac{\eta \cdot (1 + e_y)}{\mu} \right) \right) \\
 & + \left( \frac{1}{2} \eta \cdot (1 - e_y) \right) \cdot (1 - (\eta \cdot (1 - e_y))) = e_x \cdot \eta
 \end{aligned}$$

$$(2.36) \quad e_X = 1 - \eta \frac{[(1 + e_Y)^2 + (1 - e_Y)^2 \mu]}{2\mu}$$

The interaction curve for an exemplary case of uneven soil capacities, corresponding to the cases “weak” and “strong” as in section 2.2, is shown in Fig. 4b, while Fig. 4a shows it for both cases, separately.

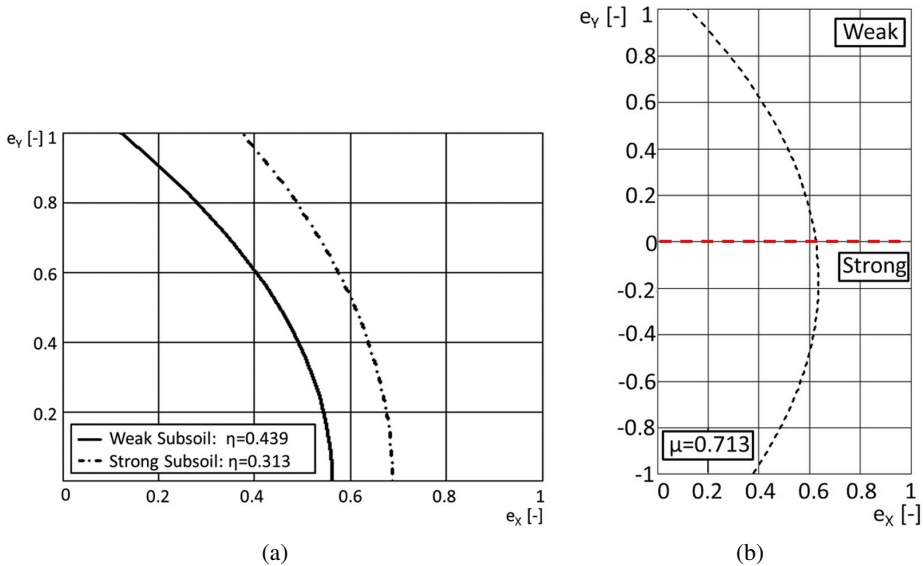


Fig. 4. Comparison of interaction curves for a case of uneven bearing capacity treated: a) separately, as for two cases b) as one, accordingly to Eq. (2.36)

### 3. 3D FEM model

#### 3.1. Introductory information

To verify results of the Analytical Model from section 2.4, a three-dimensional FE model was created in the ZSoil.PC v.20 software system [28]. It is capable to fully simulate the interaction of the caterpillar track machine with the subsoil until achieving the ultimate limit state. By performing computations using the 3D FEM model, it is possible to consider the overlapping of the impact zones of individual caterpillars on the subsoil (omitted in the 3D FEM Model  $\frac{1}{2}$  [22] and in the Analytical Model). The 3D FEM model contains layered subsoil (Mohr-Coulomb elastic-plastic) and two caterpillar tracks (elastic continuum). EAS 8 node brick elements (with two extra strain modes) were used to discretize subsoil. These elements are known as locking free (have optimal constraint to free degrees of freedom ratio) and therefore can be used to carry out limit state analyses, see [31] for details.

Additionally, high-rigidity beam elements were used to connect the two tracks. Each track is modelled as a stiff beam plus stiff elastic element (with Young's modulus significantly higher compared to other elements). On the contact surface of the track with the ground, "contact interface" elements were used. In ZSoil contact interface element may be placed only between continuum elements, that is why adding continuum el. was necessary. To increase the accuracy of the ZSoil model, directly under the tracks FE mesh is densified and a "mesh tying" interface [31] is used between zones of grids of different densities. Again, in each of the analysed models, the data (total weight, geometry of the track system) were used as for the Bauer BG20H/BT60 piling machine. Due to the universality of the computer modelling, there are no contraindications for their use in the case of other tracked construction machines (e.g. drilling rigs, construction cranes, excavators, etc.).

It was assumed that the track system was loaded initially with a constant vertical force  $Q$  being the total weight of the machine acting at the center of the system. Then, the simulation process is carried out incrementally by imposing rotations, i.e. pair of rotational D.o.F ( $\phi_X$ ,  $\phi_Y$ ) at a central nodal point of the almost infinitely stiff beam connecting two tracks. Kinematic control, for the each case of prescribed angle  $\theta_i$  ( $\theta_1 = 0^\circ$ ;  $\theta_2 = 15^\circ$ ;  $\theta_3 = 30^\circ$ ;  $\theta_4 = 45^\circ$ ;  $\theta_5 = 60^\circ$ ;  $\theta_6 = 75^\circ$ ;  $\theta_7 = 90^\circ$ ), indicating inclination direction, was as follows:

$$\phi_X = \phi \cdot \cos \theta, \quad \phi_Y = \phi \cdot \sin \theta,$$

where  $\phi$  is a gradually increasing rotation multiplier.

For each step, reactions at the constrained D.o.F, being a pair of moments ( $M_X$ ,  $M_Y$ ) are noted. Each simulation is continued incrementally until the moments in which reactions stabilize, reaching the values  $M_{X, \max}$ ,  $M_{Y, \max}$ . This corresponds to the loss of stability of the system. N.B., this effect was obtained smoothly under described kinematic control, while it was hardly feasible with applied static control, i.e. loading by moments  $M_X$ ,  $M_Y$ . Two models with assumed soil parameters are shown in Fig. 5 and Fig. 6.

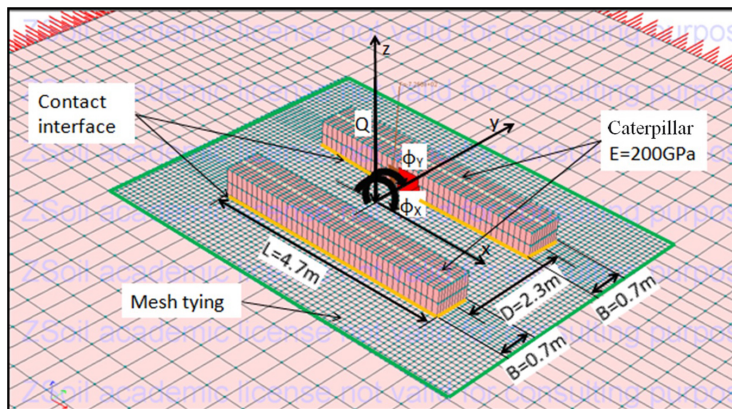


Fig. 5. General view of the 3D FEM Model

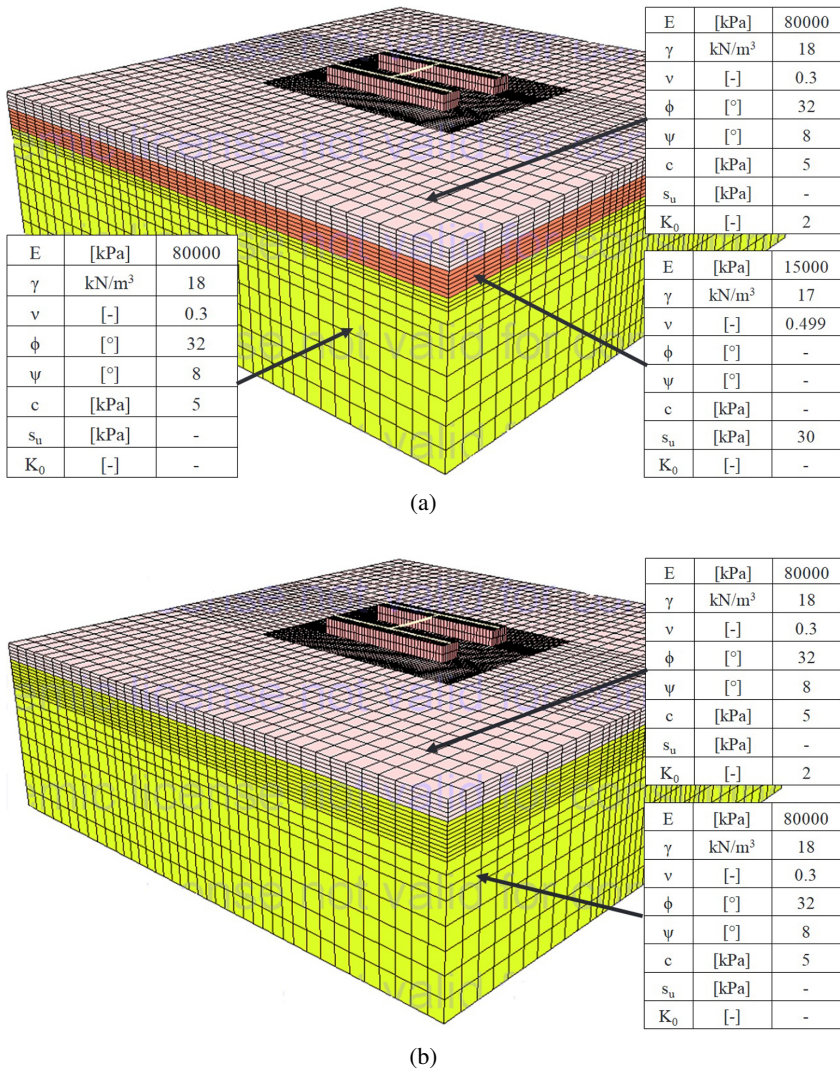


Fig. 6. 3D FEM models: a) Model 1 – “weak”, b) Model 2 – “strong”

### 3.2. Results

The most important result of the simulation obtained from the 3D FEM model are paths  $(\phi_X, M_X)$  and  $(\phi_Y, M_Y)$  as well pair of moments  $M_{X.\max,\theta}, M_{Y.\max,\theta}$  at the moment of the stability loss of the subsoil, read for each path  $\theta$ . Examples of graphs of these are shown in Fig. 7.

A view of rescaled deformations together with plasticization zones at a final stage of the 3D FEM modelling for the subsoil of “weak” case are shown in Fig. 8.

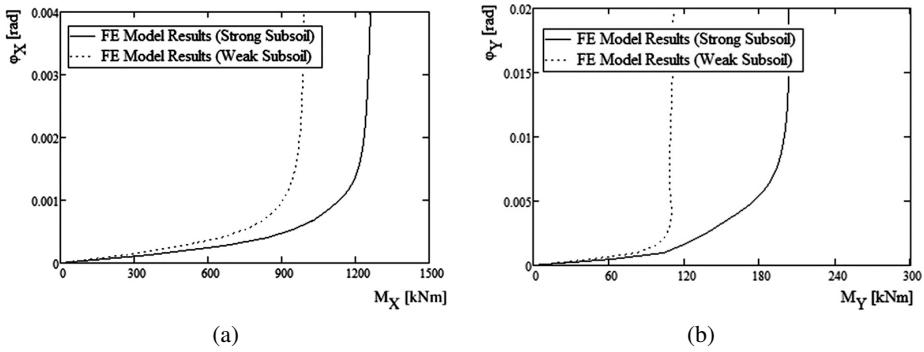


Fig. 7. Results of 3D FEM model. Example of “weak” subsoil: a)  $\varphi_X(M_X)$  for  $\theta_2 = 15^\circ$ , b)  $\varphi_Y(M_Y)$  for  $\theta_2 = 15^\circ$

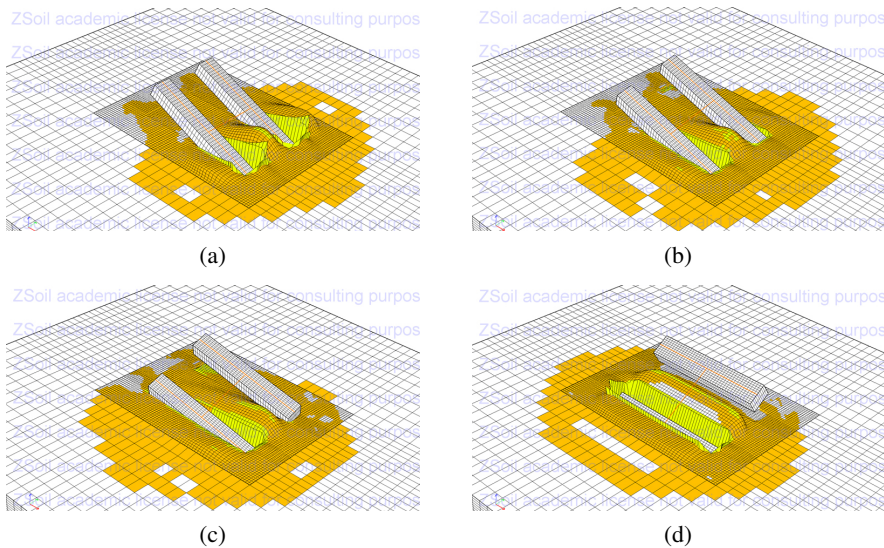


Fig. 8. Deformation (rescaled) for the 3D FEM model with the designation of plastic zones (Model 1 – “weak”): a)  $\theta_1 = 0^\circ$ , b)  $\theta_3 = 30^\circ$ , c)  $\theta_5 = 60^\circ$ , d)  $\theta_7 = 90^\circ$

### 4. Comparison of the interaction curves

For each of loading paths with different  $\theta$  dimensionless eccentricities corresponding to the pair of ultimate moments  $M_{X,max,\theta}$ ,  $M_{Y,max,\theta}$  obtained from the 3D FEM model are evaluated as:

$$(4.1) \quad e_{X,max,\theta} = \frac{2 \cdot M_{X,max,\theta}}{Q \cdot L}$$

$$(4.2) \quad e_{Y,max,\theta} = \frac{2 \cdot M_{Y,max,\theta}}{Q \cdot D}$$

They consist the points of interaction curves in space  $(e_X, e_Y)$  obtained numerically. Figure 9 shows a comparison of these interaction curves with those obtained on the basis of the results obtained from the different variants of Analytical Model.

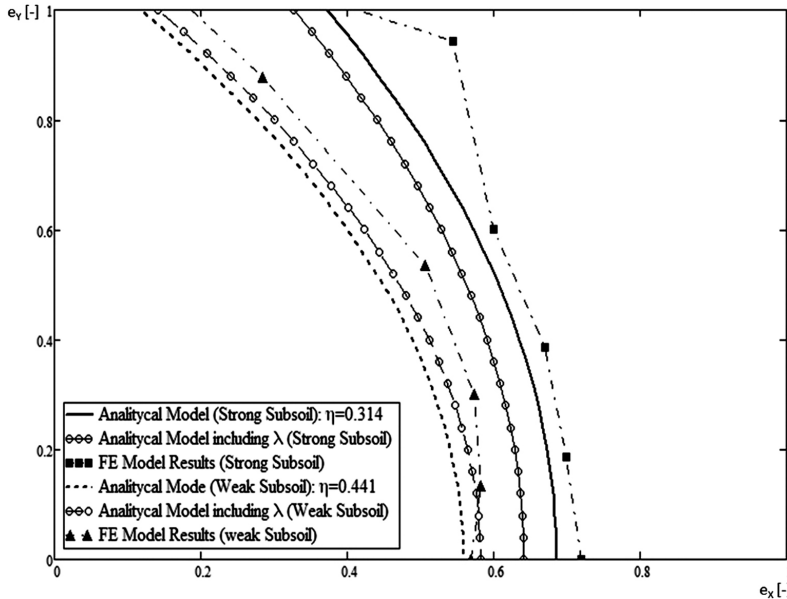


Fig. 9. Interaction curves for different dimensionless eccentricities  $e_X, e_Y$  and the two subsoil cases “weak” and “strong”

In the analysed cases, the Analytical Model based on the 2D estimation of the bearing capacity corresponds qualitatively to the results of the 3D FEM model. Some quantitative discrepancies are due to differences in the failure mechanism. In the 3D FEM model, in simple terms, the destruction takes place by pressing a rotating stamp. On the other hand, the Analytical Model assumes even pressing (without rotation) of the stamp into the soil substrate. The second reason is the simplified distribution of contact stresses assumed in the Analytical Model (Fig. 1), neglecting the increase in stress at the end of the caterpillar. However, it should be acknowledged that the presented Analytical Model gives more conservative results (on the safety side) than those derived from the 3D FEM model (elastic-plastic model of the subsoil loaded with a rigid track).

## 5. Final conclusions

This paper compares the two possible approaches (Analytical Model and 3D FEM model) to determine the stability of a heavy construction machine considering the interaction of a heavy construction machine – working platform – weak soil foundation.

In the recent work the Analytical Model has been enhanced with taking into account the dependency of subsoil load capacity with a length of loaded zone, furthermore of different soil condition under each track and consideration of the second failure mechanism in 3D space.

The main disadvantage of the three-dimensional computer models is that their execution and analysis necessary to create interaction curves ( $e_X$ ,  $e_Y$ ), requires tracing a full path until reaching the ultimate limit state. This, in all cases, is extremely time consuming, what makes the use of three-dimensional models (e.g., the 3D FEM Model  $\frac{1}{2}$  [21–23] presented in earlier works by researchers or the currently presented 3D FEM model) difficult to accept in engineering practice. Therefore, one of the elements of the research carried out by the authors of this article was to create an approximate but equivalent method of analysis (Analytical Model), which in the future may be the basis for a design procedure based on readily available data such as load capacity subsoil in a state of 2D plane strain deformation. The application of basic Analytical Model in design algorithm was described in detail in the work [22]. According to the authors, the presented Analytical Models, with or without enhancements contained in this article, have a chance to find application in design practice due to the presentation of a complex problem by means of a synthetic combination of several theories known for years. In addition, the Analytical Models do not require complex and long-term computer modelling as hand calculation yields results instantly. The results obtained from the full 3D computer simulation were compared with the Analytical Models developed by the researchers, demonstrating quantitative and qualitative compliance, which ultimately confirms their correctness. In authors opinion, this issue, provides similar level of accordance with reality as in the other practical geotechnical problems (load capacity of foundation or pressure on retaining structures). Of course experimental investigation, for example real scale in-situ tests can be also useful in confirmation of the theory, but first of all they would require very thorough identification of given subsoil data.

The authors hope that the results presented in this paper, mainly easy obtainable interaction curves, may be used as a reference point in solving the problem of stability analysis of heavy tracked machines operating on weak ground. However, it must be said that in the proposed Analytical Model and referential 3D FEM model only the mechanical framework of the analysed issue is given. It should not be considered in the context of exhausting the research topic, as some kind of reliability analysis leading to establishing proper safety factors is needed.

## References

- [1] H.J. Burd and S. Frydman, "Bearing capacity of plane-strain footings on layered soils", *Canadian Geotechnical Journal*, vol. 34, no. 2, pp. 241–253, 1997, doi: [10.1139/cgj-34-2-241](https://doi.org/10.1139/cgj-34-2-241).
- [2] R.L. Michałowski and L. Shi, "Bearing capacity of footings over two-layer Foundation soils", *Journal of Geotechnical Engineering*, vol. 121, no. 5, pp. 421–428, 1995, doi: [10.1061/\(ASCE\)0733-9410\(1995\)121:5\(421\)](https://doi.org/10.1061/(ASCE)0733-9410(1995)121:5(421)).
- [3] M. Chwała, W. Puła, and M. Kawa, "Probabilistic bearing capacity evaluation for two-layered soil", in *Proceedings of the 7th International Symposium on Geotechnical Safety and Risk*. ISGSR, 2019, pp. 297–302, doi: [10.3850/978-981-11-2725-0-IS10-4-cd](https://doi.org/10.3850/978-981-11-2725-0-IS10-4-cd).
- [4] M. Chwała and W. Puła, "Evaluation of shallow foundation bearing capacity in the case of a two-layered soil and spatial variability in soil strength parameters", *PLoS ONE*, vol. 15, no. 4, 2020, doi: [10.1371/journal.pone.0231992](https://doi.org/10.1371/journal.pone.0231992).

- [5] Ł. Zaskórski, W. Puła, and D.V. Griffiths, "Bearing capacity assessment of a shallow foundation on a two-layered", in *Geo-Risk 2017 – Reston: American Society of Civil Engineers*. ASCE, 2017, pp. 468–477, doi: [10.1061/9780784480724.042](https://doi.org/10.1061/9780784480724.042).
- [6] M.J. Kenny and K.Z. Andrawes, "The bearing capacity of footings on a sand layer over lying soft clay", *Geotechnique*, vol. 47, no. 2, pp. 339–345, 1997, doi: [10.1680/geot.1997.47.2.339](https://doi.org/10.1680/geot.1997.47.2.339).
- [7] S.S. Eshkevari, A.J. Abbo, and G. Kouretzis, "Bearing capacity of strip footings on sand over clay", *Canadian Geotechnical Journal*, vol. 56, no. 5, pp. 699–709, 2018, doi: [10.1139/cgj-2017-0489](https://doi.org/10.1139/cgj-2017-0489).
- [8] Z. Mróz and A. Drescher, "Limit plasticity approach to some cases of flow of bulk solids", *Journal of Engineering for Industry*, vol. 91, no. 2, pp. 357–364, 1969, doi: [10.1115/1.3591573](https://doi.org/10.1115/1.3591573).
- [9] P. Purushothamaraj, B.K. Ramiah, and K.N. Venkatakrishna Rao, "Bearing capacity of strip footings in two layered cohesive-friction soils", *Canadian Geotechnical Journal*, vol. 11, no. 1, pp. 32–45, 1974, doi: [10.1139/t74-003](https://doi.org/10.1139/t74-003).
- [10] V. Khatri, J. Kumar, and S. Akhtar, "Bearing capacity of foundations with inclusion of dense sand layer over loose sand strata", *International Journal of Geomechanics*, vol. 17, no. 10, pp. 601–618, 2017, doi: [10.1061/\(ASCE\)GM.1943-5622.0000980](https://doi.org/10.1061/(ASCE)GM.1943-5622.0000980).
- [11] M. Huang and H. Qin, "Upper-bound multi-rigid-block solutions for bearing capacity of two-layered soils", *Computers and Geotechnics*, vol. 36, no. 3, pp. 525–529, 2009, doi: [10.1016/j.compgeo.2008.10.001](https://doi.org/10.1016/j.compgeo.2008.10.001).
- [12] W.F. Chen and H.L. Davidson, "Bearing capacity determination by limit analysis", *Journal of the Soil Mechanics and Foundations Division*, vol. 99, no. 6, pp. 433–449, 1973, doi: [10.1061/JSFEAQ.0001887](https://doi.org/10.1061/JSFEAQ.0001887).
- [13] D.M. Dewaikar and B.G. Mohapatra, "Computation of bearing capacity factor Ny-Prandtl's mechanism", *Soils and Foundations*, vol. 43, no. 3, pp. 1–10, 2003, doi: [10.3208/sandf.43.3\\_1](https://doi.org/10.3208/sandf.43.3_1).
- [14] E. Detournay and A. Drescher, "Limit load in translational materials for associated and non-associated materials", *Géotechnique*, vol. 43, no. 3, pp. 443–456, 1993, doi: [10.1680/geot.1993.43.3.443](https://doi.org/10.1680/geot.1993.43.3.443).
- [15] H. Michalak and P. Przybysz, "Subsoil movements forecasting using 3D numerical modeling", *Archives of Civil Engineering*, vol. 67, no. 1, pp. 367–385, 2021, doi: [10.24425/ace.2021.136478](https://doi.org/10.24425/ace.2021.136478).
- [16] A.J. Valsangkar and G.G. Meyerhof, "Experimental study of punching coefficients and shape", *Canadian Geotechnical Journal*, vol. 16, no. 4, pp. 802–805, 1979, doi: [10.1139/t79-086](https://doi.org/10.1139/t79-086).
- [17] R.L. Michalowski, "Limit analysis of weak layers under embankments", *Soils and foundations*, vol. 33, no. 1, pp. 155–168, 1993, doi: [10.3208/sandf1972.33.155](https://doi.org/10.3208/sandf1972.33.155).
- [18] M. Chwała and M. Kawa, "Random failure mechanism method for assessment of working platform bearing capacity with a linear trend in undrained shear strength", *Journal of Rock Mechanics and Geotechnical Engineering*, vol. 13, no. 6, pp. 1513–1530, 2021, doi: [10.1016/j.jrmge.2021.06.004](https://doi.org/10.1016/j.jrmge.2021.06.004).
- [19] A. Johari, A. Sabzi, and A. Gholaminejad, "Reliability analysis of differential settlement of strip footings by stochastic response surface method", *Iranian Journal of Science and Technology*, vol. 43, no. 1, pp. 37–48, 2019, doi: [10.1007/s40996-018-0114-3](https://doi.org/10.1007/s40996-018-0114-3).
- [20] A. Johari, S. M. Hosseini, and A. Keshavarz, "Reliability analysis of seismic bearing capacity of strip footing by stochastic slip lines method", *Computers and Geotechnics*, vol. 91, pp. 203–217, 2017, doi: [10.1016/j.compgeo.2017.07.019](https://doi.org/10.1016/j.compgeo.2017.07.019).
- [21] A. Urbański, A. Truty, and M. Richter, "Stability of drilling rigs moving on a weak subsoil. Theoretical formulation and selected case studies", *Engineering Structures*, vol. 184, pp. 524–534, 2019, doi: [10.1016/j.engstruct.2019.01.111](https://doi.org/10.1016/j.engstruct.2019.01.111).
- [22] A. Urbański and M. Richter, "Stability analysis of heavy machinery moving on weak subsoil. Analytical solution", *Engineering Structures*, vol. 241, 2021, doi: [10.1016/j.engstruct.2021.112152](https://doi.org/10.1016/j.engstruct.2021.112152).
- [23] A. Urbański and M. Richter, "Stability analysis of drilling rigs moving on a weak subsoil. Selected case studies", *Archives of Civil Engineering*, vol. 66, no. 2, pp. 303–319, 2020, doi: [10.24425/ace.2020.131811](https://doi.org/10.24425/ace.2020.131811).
- [24] BAUER Maschinen GmbH, "BG 20 H. Großdrehbohrgerät. Rotary Drilling Rig", 2015.
- [25] P. Wriggers, *Computational contact mechanics*. Springer, 2006.
- [26] M. Kuczma, "A viscoelastic-plastic model for skeletal structural systems with clearances", *Computer Assisted Mechanics and Engineering Sciences*, vol. 6, pp. 83–106, 1999.
- [27] Ch. Su, et al., "Combining finite element and analytical methods to contact problems of 3D structure on soft foundation", *Mathematical Problems in Engineering*, vol. 2020, 2020, doi: [10.1155/2020/8827681](https://doi.org/10.1155/2020/8827681).



- [28] EN 1997-1 Eurocode 7: Geotechnical design – Part 1. ISO, 2004.
- [29] J.E. Bowles, *Foundations analysis and design*. McGraw-Hill Publishing Company, New York, 1996.
- [30] Z. Szypcio and K. Dołżyk, “The bearing capacity of layered subsoil”, *Studia Geotechnica et Mechanica*, vol. 28, no. 1, pp. 45–60, 2006.
- [31] “ZSoil Manual”. [Online]. Available: <https://zsoil.com/zsoil-manual/>. [Accessed: 25 Apr. 2023].

## **Analiza stateczności ciężkich maszyn budowlanych poruszających się po podłożu słabonośnym. Model 3D MES vs. modele analityczne**

**Słowa kluczowe:** inżynieria geotechniczna, krzywe interakcji, interakcja podłoże gruntowe – maszyna budowlana, model 3D MES, modele analityczne, platforma robocza

### **Streszczenie:**

W artykule autorzy przedstawiają rozszerzenie zakresu dotychczas przeprowadzonych badań o pełną trójwymiarową symulację komputerową (metodą elementów skończonych), która uwzględnia interakcję między: gąsienicowym układem jezdny – platformą roboczą – podłożem gruntowym. W artykule przedstawiono model komputerowy uwzględniający układ jezdny dwóch gąsienic maszyny budowlanej znajdujących się na podłożu gruntowym, sprężysto-plastycznym, przy warunkach plastyczności Mohra-Coulomba, pozwalający na komputerową symulację zachowania się układu aż do osiągnięcia stanu granicznego nośności. Wyniki powyższego modelu komputerowego traktuje się jako odniesienie dla uproszczonych Modeli Analitycznych szacowania stanu granicznego, które mogą być wykorzystane w procedurach projektowych. Najważniejszymi wynikami wynikającymi z Modelu Analitycznego są proste krzywe interakcji, w przestrzeni momentów działających na układ gąsienicowa maszyna budowlana – podłoże gruntowe, ograniczające zakres działania przy danych parametrach podłoża gruntowego.

Received: 2023-04-27, Revised: 2023-10-31